Science of the Total Environment 806 (2022) 151201

Contents lists available at ScienceDirect

Science of the Total Environment

journal homepage: www.elsevier.com/locate/scitotenv

Effective concentration signature of Zn in a natural water derived from various speciation techniques

Kevin Rosales-Segovia [a], Jordi Sans-Duñó [a], Encarna Companys [a], Jaume Puy [a], Berta Alcalde [b], Enriqueta Anticó [b], Clàudia Fontàs [b], Josep Galceran [a,*]

[a] Departament de Química. Universitat de Lleida, and AGROTECNIO-CERCA, Rovira Roure 191, 25198 Lleida, Catalonia, Spain
[b] Departament de Química, Universitat de Girona, Maria Aurèlia Capmany 69, 17003 Girona, Catalonia, Spain

HIGHLIGHTS

- The concept of effective concentration signature is proposed.
- Complementary information from various techniques can yield lability degrees.
- The concept of the labile concentration c_{LASV} is introduced.

GRAPHICAL ABSTRACT

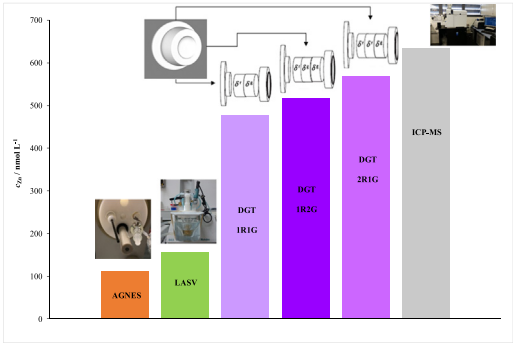

ARTICLE INFO

Article history:
Received 9 July 2021
Received in revised form 9 October 2021
Accepted 20 October 2021
Available online 23 October 2021

Editor: Damia Barcelo

Keywords:
Analytical techniques
Diffusive boundary layer
Bioavailability
Lability
Complexation

ABSTRACT

The uptake of nutrients or toxicants by different organisms in aquatic systems is known to correlate with different fractions of the nutrient's or toxicant's total concentration. These fractions can be provided by different analytical techniques, from which the better correlation is expected to be found for those with a characteristic length comparable to that in the considered organism uptake. An effective concentration signature can be built up with the concentration values associated to the availability (i.e. fluxes in dynamic techniques) of the nutrient or toxicant measured by various analytical techniques with different characteristic lengths. Here, this new representation was obtained for the pool of Zn complexes in the Mediterranean stream Riera d'Osor (Girona, Catalonia, Spain) with a suite of four analytical techniques. Absence of Gradients and Nernstian Equilibrium Stripping (AGNES) and Polymer Inclusion Membrane (PIM) devices provided the free Zn concentration. Linear Anodic Stripping Voltammetry provided a labile fraction (defined here as c_{LASV}, higher than the free concentration), related to the diffusion layer scale. Diffusion Gradients in Thin-films provided higher labile fractions (known as DGT concentrations, c_{DGT}) connected to the different characteristic lengths of different configurations (e.g. one or two resin discs) longer, in any case, than that corresponding to LASV. The combination of the information retrieved by the techniques allowed to quantify lability degrees of the pool of Zn complexes and to build up the effective concentration signature for this water.

1. Introduction

Bioavailability of a metal to environmental biota depends on biological and physicochemical factors (Worms et al., 2006). Equilibrium

* Corresponding author.
E-mail address: galceran@quimica.udl.cat (J. Galceran).

https://doi.org/10.1016/j.scitotenv.2021.151201

models (such as FIAM –Free Ion Activy Model- and BLM –Biotic Ligand Model-) are suitable in many instances, but, in others, dynamic aspects (such as diffusion in the vicinity of the active surface or the dissociation rate of the metal complexes) rule the uptake (Sigg et al., 2006). Moreover, the dynamics can be modulated by the length of the path to be followed by the metal species from the bulk of the medium towards the active surface of the biota. So, no single analytical technique –applied to the medium- can claim to provide a complete description of the availability of the metal in such a medium for all organisms, because each analytical technique accesses to a window of the total information, usually related to some characteristic length of its sensor (Sigg et al., 2006; van Leeuwen et al., 2005). The more techniques (with different characteristics) contribute with their specific information, the more complete the resulting picture of the metal availability in the medium will be.

The integration of the various information has been hampered by the fact that some techniques yield concentrations (i.e. the free one or the total one), while other (dynamic) techniques yield a flux (van Leeuwen et al., 2005), which only rarely has been converted into an equivalent concentration.

Here, four speciation techniques are applied to analyse Zn in water from the Riera d'Osor stream (Girona, Spain). AGNES (Absence of Gradients and Nernstian Equilibrium Stripping)(Companys et al., 2017; Galceran et al., 2004) and PIM (Polymer Inclusion Membrane) (Almeida et al., 2012; Nghiem et al., 2006) are techniques providing –in the current conditions- the free metal ion concentration. LASV (Anodic Stripping Voltammetry with Linear scan) (Bard and Faulkner, 2001; Companys et al., 2018; Pesavento et al., 2009) and DGT (Diffusive Gradients in Thin-films) (Davison and Zhang, 1994; Galceran et al., 2021; Menegario et al., 2017) are dynamic techniques describing different labile fractions. In the case of DGT, different characteristic lengths have been explored through different configurations with one or more resin disc(s) plus one or more diffusive gel disc(s).

The main aim of this paper is to present the "*effective concentration signature*" as an integration of the measurements obtained with the different techniques, based on the comparison of the available concentrations retrieved by each one of the techniques. The key point is to convert all fluxes into equivalent concentrations. This effective concentration signature can be useful in estimating the availability of the analyte (Zn in this work) to different organisms with different thicknesses of their relevant diffusive boundary layers. This availability has to be seen as an upper limit to Zn *bioavailability*, which includes other factors such as the homeostasis of the organism (impacting on the internalization process) or competition effects from other cations (including proton) (Price et al., 2021).

Established methods of the various techniques employed in this work are not repeated here, as interested readers can find this information in the cited references and in the Supporting Information. On the other hand, details are provided about the new contributions of this paper such as: i) preliminary results with the first *in situ* application and a simple model of PIM to estimate $[Zn^{2+}]$; ii) methodology and implementation to find the lability degree of a pool of complexes with LASV; iii) introduction of the concept of c_{LASV}; iv) first application of AGNES with the rotating disc electrode (RDE) to an environmental water; v) comparison of the lability degrees from LASV and DGT with different configurations and vi) introduction of the concept of the effective concentration signature. The methodology and interpretation of results obtained here for Zn in the Mediterranean stream Riera d'Osor is a proof of concept that can be applied to other natural waters and other elements (perhaps with the use of other/additional equilibrium or dynamic techniques).

2. Material and methods

2.1. Sampling

The Riera d'Osor stream (from now on, just "Osor stream") is a tributary of the Ter river (Catalonia, Spain) from its right bank. It has been selected because of its high Zn concentration levels due to former mining activities (Antico et al., 2020; Morin et al., 2014; Navarro et al., 2015) and its low organic matter content. Deployment and sampling were performed at coordinates 41° 57′ 14" N, 2° 35′ 58″ E on 10th and 11th March 2020. Physical parameters (including temperature) have been measured at different times during these two days using an Orion Star A329 pH/ISE/Conductivity/RDO/DO Meter. Ionic strength (μ) has been calculated from conductivity (EC) using the empirical Russell equation (APHA, 1998) (EC in μS cm^{-1}, μ in mol L^{-1})

$$\mu = 1.6 \times 10^{-5} \times EC \tag{1}$$

as in previous works where AGNES was applied to non-modified freshwater samples (Chito et al., 2012; Zavarise et al., 2010).

Samples for elemental analysis were prepared *in situ* by mixing 9.98 mL of filtered (0.45 μm pore size) stream water with 20 μL of HNO_3 70%. These samples (in triplicate) were analysed for total Zn using an inductively coupled plasma mass spectrometer (ICP-MS, 7700x, Agilent Technologies, Inc.). AGNES and LASV experiments were conducted on the last grab sample from 11th March 2020 (last row in Table 1). Majoritary anions and cations (measured with ion chromatography, IC), alkalinity and Dissolved Organic Carbon (DOC) of this last grab sample were analysed in the Scientific and Technical Services of the Catalan Institute for Water Research (ICRA).

2.2. Electroanalytical techniques

In AGNES (Galceran et al., 2014), the application of a suitable deposition potential (E_1) allows –when equilibrium is reached by the end of the deposition stage- to preconcentrate Zn° homogeneously in the mercury electrode up to a factor Y (gain), according to the Nernstian equation:

$$Y = \frac{\left[Zn^0\right]}{\left[Zn^{2+}\right]} = \exp\left[-\frac{2F}{RT}\left(E_1 - E^{0'}\right)\right] \tag{2}$$

where F is the Faraday constant, R the gas constant, T the temperature and $E^{0'}$ the standard formal potential of the redox couple and E_1 the applied deposition potential. Gains $Y = 10{,}000$ and $Y = 20{,}000$ were applied (by selecting the corresponding E_1 value) for the measurement of the river sample with different deposition times t_1. Here, we have used AGNES variants 1P for the first stage and Stripping ChronoPotentiometry (SCP) for the second one (Companys et al., 2005; Parat et al., 2011; Parat et al., 2015) (see Supporting Information, SI, with details about these AGNES variants).

Due to Faraday's law, the computed faradaic stripped charge is proportional to $[Zn^0]$ and, by combining with Eq. (2), to the free Zn concentration:

$$Q = \eta_Q Y\left[Zn^{2+}\right] \tag{3}$$

The proportionality factor η_Q has been found from a calibration at the same ionic strength and temperature. Y was computed from an

Table 1
Physicochemical parameters of the sampled water in Osor. The last row, highlighted in bold, corresponds to the samples taken to the laboratory for AGNES and LASV experiments.

Day	Time	pH	T (°C)	DO (mg L^{-1})	EC (μS cm^{-1})	I (mol m^{-3})	$c_{T,\,Zn}$ (nmol L^{-1})
10/03/20	14:52	9.08	12.0	10.99	233.4	3.73	423
10/03/20	19:50	8.48	11.9	10.67	235.9	3.77	811
11/03/20	10:00	8.29	9.9	11.07	251.9	4.02	673
11/03/20	15:00	9.08	15.9	10.47	238.9	3.82	434
11/03/20	**18:45**	**8.58**	**12.3**	**10.24**	**246.8**	**3.95**	**633**

auxiliary Differential Pulse Polarography experiment (Companys et al., 2017; Zavarise et al., 2010) at ionic strength 0.1 mol L^{-1} and using the correction indicated by Eq. (2) in ref. (Galceran et al., 2014) as shown in SI-2. In this way, AGNES provided $[Zn^{2+}]$ of the sampled solution.

In LASV, the faradaic stripped charge ($Q_{faradaic}$) essentially provides the Zn^0 previously accumulated during a deposition time ($t_{1,a}$), along which we can assume that a steady-state flux, under perfect sink conditions, holds (Companys et al., 2018):

$$Q_{faradaic} = 2FAJt_{1,a} \quad (4)$$

where A is the area of the mercury electrode (which in the case of the rotating disc electrode was taken from the technical sheet as 3.098 mm^2) and J the steady-state flux. Here, we have used a linear scan at progressively less negative potentials for the stripping stage, but one could use a fixed stripping current and record the potential (i.e. in a Stripping ChronoPotentiometry, SCP, mode) (van Leeuwen et al., 2005). In any case, a labile flux J can be determined.

AGNES and LASV voltammetric measurements were carried out with Eco Chemie Autolab PGSTAT101 and μAutolab Type III potentiostats attached to Metrohm 663VA stands, being controlled from a computer by means of the NOVA 1.11 and GPES 4.9 softwares. The working electrode was a thin mercury film plated on a rotating glassy carbon electrode (2 mm diameter, Metrohm) as in previous applications of AGNES to synthetic solutions (Pinheiro et al., 2020; Rocha et al., 2010). The electrode was prepared daily following a procedure adapted from (Monterroso et al., 2003; Rotureau et al., 2019). The reference electrode was a Ag/AgCl /3 mol L^{-1} KCl, encased in a jacket containing 0.1 mol L^{-1} KNO_3 and the counter electrode was a glassy carbon one. A glass combined electrode (Hach) was attached to an Orion Dual ion Analyzer (Thermo) and introduced in the cell to control the pH. For both, AGNES and LASV, a specific purging system with a mixture of N_2/CO_2 was used to remove oxygen while keeping the pH constant (Lao et al., 2015; Pei et al., 2000). The sample was measured in a teflon cell provided by Metrohm coupled to a glass jacket thermostated at 12.3 °C (the temperature of the stream at the last grab sampling) by means of a recirculating bath. An aliquot of the sampled solution was left overnight to equilibrate Zn adsorption onto the walls, then the cell was rinsed with more sample solution and fill with it (Jansen et al., 1998).

The deposition potential used in LASV was −1.200 V (during a time $t_{1,a}$ from 15 s to 300 s in the determination of the diffusion layer thickness, and just 300 s in the calibrations and sample measurements), followed by a linear scan at 0.0198 V s^{-1}. Lability is independent from the particular deposition potential (as long as it corresponds to diffusion limited conditions).

2.3. DGT

The diffusive gel is a polyacrylamide cross-linked disc made of a commercial agarose derivative often designated as APA. The resin layer contains a powder (Chelex 100) incorporated into a gel matrix (APA gel). Other details on the preparation and handling of DGT devices can be found elsewhere (Sans-Duñó et al., 2021).

Three DGT configurations have been used here: i) one resin disc and one diffusive gel disc (code 1R1G); ii) two resin discs and one gel disc (2R1G) and iii) one resin disc and two gel discs (1R2G). Twelve DGTs containing 1R1G, seven DGT containing 2R1G and seven DGT containing 1R2G were deployed. Deployment times for different configurations were: 5 h 47 min (1R1G), 19 h 57 min (1R1G), 28 h 37 min (1R1G), 166 h 22 min (1R1G), 28 h (2R1G), 166 h 7 min (2R1G), 28 h 25 min (1R2G) and 165 h 52 min (1R2G). The longest time corresponded to a set of devices left until March16th 2020.

DGT blanks (prepared as 1R1G, but not deployed) were transported from our laboratory to the field (and back) in a sealed plastic bag alongside DGT devices used for deployment. This blank accumulation is subtracted from the accumulated moles in DGT devices deployed in Osor stream.

The clamps used as support structure for DGT deployment were washed the day before deployment with ultra-purified water and nitric acid.

From the slope (s) of the linear regression of the plot accumulated moles vs. time (e.g. see Fig. 2), c_{DGT} is calculated as:

$$c_{DGT} = \frac{s\Delta g}{D^g_{Zn}A} \quad (5)$$

where D^g_{Zn} is the diffusion coefficient of Zn across the gel disc (4.20×10^{-10} m^2 s^{-1}, reported by DGT Research), A is the exposed area (3.14 mm^2) and Δg is the aggregate thickness of the diffusive gel(s) plus filter plus an estimated diffusive boundary layer (DBL) of 0.3 mm (Levy et al., 2012; Warnken et al., 2007). The thicknesses of an individual diffusive gel, resin and filter are $\delta^g = 0.629$ mm, $\delta^r = 0.4$ mm and $\delta^f = 0.150$ mm, respectively.

3. Theory

3.1. The lability degree

The lability degree ξ is defined (Galceran et al., 2001; Puy and Galceran, 2017) as the fraction of the current contribution of the complexes with respect to the maximum possible contribution if all complexes were fully labile:

$$\xi \equiv \frac{J - J_{inert}}{J_{labile} - J_{inert}} \quad (6)$$

where J is the flux in the sampling measurement (where ξ is to be determined). J_{inert} indicates the flux that would be obtained if the complexes were fully inert (i.e. if the flux was only sustained by the free metal concentration, with no dissociation from the complex). J_{labile} indicates the flux that would be obtained if the complexes were fully labile (i.e. no kinetic limitation to reach equilibrium between the Zn species in solution).

3.2. c_{DGT} interpreted in terms of real species and lability degrees

As shown elsewhere (Baeyens et al., 2018; Galceran et al., 2021; Galceran and Puy, 2015; Zhao et al., 2020), the operationally defined DGT concentration, c_{DGT}, can be expressed in terms of the contribution of the free metal plus those of the different complexes which are weighted by their normalized diffusion coefficients (ε_j) and their lability degrees (ξ_j). If there are h parallel complexes with the ligands ^jL,

$$c_{DGT} = \left[Zn^{2+}\right] + \sum_{j=1}^{h} \xi_j \varepsilon_j \left[Zn^jL\right] \quad (7)$$

where the normalized diffusion coefficients are

$$\varepsilon_j = \frac{D_{Zn^jL}}{D_{Zn}} \quad (8)$$

In Eq. (7) one assumes that the ratio of diffusion coefficients is the same in water (i.e. in the DBL) as in the gel phase or the filter.

3.3. Measuring lability degrees in LASV with RDE

Given the proportionality between the faradaic charge and flux (when a common deposition time is taken) in Eq. (4), ξ from Eq. (6), can be written as

$$\xi = \frac{Q - Q_{inert}}{Q_{labile} - Q_{inert}} \quad (9)$$

where all charges are assumed to be faradaic.

To estimate Q_{inert} and Q_{labile}, we use a "calibration" where, essentially, we measured the total charge in synthetic solutions with just Zn (at low pH) in supporting electrolyte (KNO_3 0.00395 mol L^{-1}) with a constant deposition time $t_{1,a}$ and total Zn concentrations 7.0×10^{-7}, 2.0×10^{-6} and 7.0×10^{-6} mol L^{-1}. In these pH conditions, all Zn species can be considered as mobile and labile, as if all Zn was free. Due to a fixed intercept (probably from a capacitive charge), the total charge in the calibration can be summarized as

$$Q_{calib} = \frac{nFAD_{Zn}t_{1,a}}{\delta_{Zn}}\left[Zn^{2+}\right] + b = s\left[Zn^{2+}\right] + b \quad (10)$$

From Eq. (10), we can determine s and b. Discounting b from the total measured charge in the water sample, we can find the faradaic charge Q to be used in (9) as $Q = s[Zn^{2+}]$. δ_{Zn} is the effective diffusion layer in the rotating disc electrode system with no relevant Zn complexation.

The "inert" faradaic charge Q_{inert} can be identified with the faradaic charge that would have been measured in the calibration experiment with a total metal concentration equal to that of free Zn in the sample (all with a common fixed deposition time).

$$Q_{inert} = s\left[Zn^{2+}\right] \quad (11)$$

where $[Zn^{2+}]$ is the free concentration in the studied sample (and known from another technique) and s is determined from the "calibration".

For the fully labile case, in excess of ligand conditions, a theoretical extension of Eq. (10) can be derived (Serrano et al., 2003):

$$Q_{labile} = \frac{nFA\bar{D}t_{1,a}}{\bar{\delta}}c_{T,Zn} \quad (12)$$

where $\bar{D}$ is an average diffusion coefficient. For instance, in a system with just one complex ZnL (whose charge is omitted for simplicity), it can be written as:

$$\bar{D} = \frac{\left[Zn^{2+}\right] + \varepsilon[ZnL]}{c_{T,Zn}}D_{Zn} \quad (13)$$

$\bar{\delta}$ is the effective diffusion layer in this labile system and is proportional to $\bar{D}^{1/3}$, i.e. the diffusion layer also depends on the diffusion coefficients of the diffusing species (Pinheiro and van Leeuwen, 2001; Pohl et al., 1998). As the effective diffusion layer δ_{Zn} depends on $D_{Zn}^{1/3}$, as shown in eq. (9.3.25) of reference (Bard and Faulkner, 2001) (with other factors such as the rotating speed being the same for both $\bar{\delta}$ and δ_{Zn}),

$$\bar{\delta} = \delta_{Zn}\left(\frac{\bar{D}}{D_{Zn}}\right)^{1/3} = \delta_{Zn}\left(\frac{\left[Zn^{2+}\right] + \varepsilon[ZnL]}{c_{T,Zn}}\right)^{1/3} \quad (14)$$

(see also Appendix in ref. (Tolmachev and Scherson, 1999)).

Q_{labile} can be obtained by combining Eqs. (12) and (14),

$$Q_{labile} = s\,c_{T,Zn}\left(\frac{\left[Zn^{2+}\right] + \varepsilon[ZnL]}{c_{T,Zn}}\right)^{2/3} \quad (15)$$

where $c_{T,Zn}$ is the total concentration in the sample (e.g. provided from elemental analysis).

Once Q, Q_{inert} and Q_{labile} are known, as described in previous paragraphs, ξ for LASV (denoted from now on as ξ_{LASV}) can be computed with Eq. (9).

4. Results and discussion

4.1. Water characteristics

Table 1 gathers measured parameters in the sampled water. The total Zn concentration for the sample analysed with AGNES and LASV (from 3 replicates: 6.36×10^{-7}, 6.31×10^{-7} and 6.31×10^{-7} mol L^{-1}) was 6.33×10^{-7} mol L^{-1}. An accurate analysis of the error for the ICP-MS measurement yielded 1.32×10^{-9} mol L^{-1}. For the last grab sample, DOC = 2.03 mg C L^{-1}, alkalinity = 75.5 mg $CaCO_3$ L^{-1} and $c_{T,Zn} = 6.33 \times 10^{-7}$ mol L^{-1}.

Speciation in the last sample has been estimated with the program Visual Minteq (VM) to obtain guidelines on the impact of organic complexation and the order of magnitude of the free fraction of Zn. Dissolved Organic Matter has been modelled using NICA-Donnan, considering a factor DOC to DOM of 1.65 which is an average value based on results for lakes and streams from the Swedish environmental network (Sjostedt et al., 2010) and assuming that all DOM corresponds to fulvic acid. The total concentration of carbonates introduced as an input comes from the alkalinity measured in the Osor stream sample. The VM input parameters (corresponding to ionic chromatography, ICP-MS, etc. information obtained on the last grab sample) are shown in Table SI-1 in the Supporting Information, together with pH = 8.584, T = 12.3 °C and considering it as a closed system (i.e. the partial pressure of CO_2 is not fixed). The speciation results (see Table SI-2) predict a small free Zn fraction (192 nmol L^{-1}, around 32.6% of the total), a large fraction of small inorganic complexes (around 65.8%, mainly Zn $(OH)_2$ and $ZnCO_3$) and a negligible fraction of large organic complexes (1.1%), as in other Mediterranean waters (Sierra et al., 2017).

4.2. Free Zn concentration with AGNES

The variant AGNES-SCP with TMF-RDE (Thin Mercury Film on the Rotating Disc Electrode) applying Y = 10,000 and Y = 20,000 (to the last grab sample taken from Osor stream on 11th March 2020) showed equilibrium conditions for deposition times from 400 s on, as seen in Fig. 1. These 400 s are consistent with the general rule, derived in this work from the collapse of normalized trajectories in a synthetic solution at different gains (details not shown), for the deposition time (in TMF-RDE) needed when only free Zn contributes to the accumulation:

$$t_1 - t_w = 0.008 \times Y \quad (16)$$

where t_w stands for the waiting or resting time applied at the end of the deposition stage.

The measured free concentrations in three independent analyses of the last grab sample were 127, 101 and 105 nmol L^{-1}, which averages to $[Zn^{2+}]$ = 111 nmol L^{-1} and compares satisfactorily with VM estimation (192 nmol L^{-1}) in Table SI-2. From now on, the experimental value of AGNES is taken as the free Zn concentration for further computations, given the uncertainties in VM computations (e.g. inaccuracies in the used stability constants and lack of $\Delta H°$ in the default database to account for the temperature impact on the stability constants of some majoritary species).

4.3. Labile concentrations and lability degrees with DGT of different configurations

As seen in Fig. 2, DGT accumulations grow linearly with deployment time. c_{DGT} computed with Eq. (5) yielded $4.76(\pm0.23) \times 10^{-7}$ mol L^{-1} (1R1G), $5.17(\pm0.03) \times 10^{-7}$ mol L^{-1} (1R2G) and $5.68(\pm0.06) \times 10^{-7}$ (2R1G). Increasing the number of diffusive gel discs decreases the

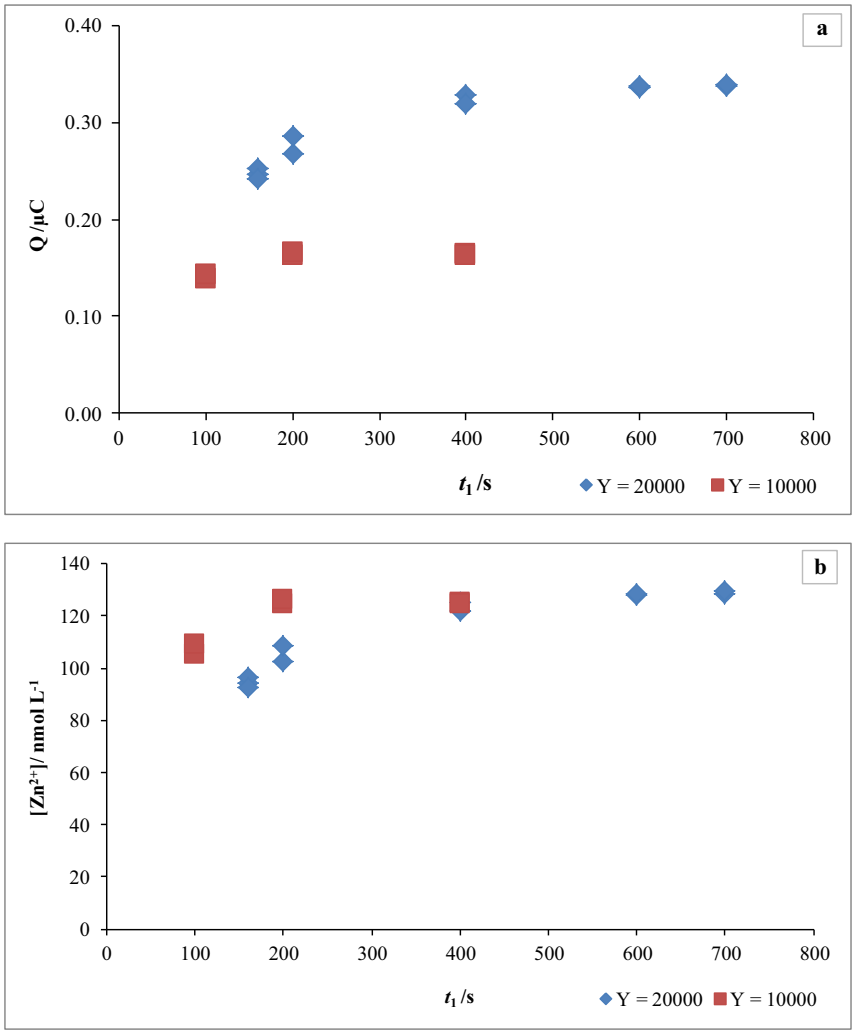

Fig. 1. Time course results (trajectories) in the application of AGNES to Osor stream water (pH = 8.5; T = 12.3 °C) showing the desired stabilization and Nernstian behaviour at sufficiently long deposition times (t_1). Panel a: Charge representation; Panel b: Concentration representation. Red square stands for Y = 10,000; while blue diamond for Y = 20,000.

accumulation, because the analyte has to arrive from further away. Increasing the number of resin discs increases the accumulation, because they drive partially labile complexes to dissociate within them. Comparing 1R1G with 1R2G, c_{DGT}-values obtained are consistent with the rule that larger diffusion domains allow to sense a larger labile fraction. In 2R1G, the percentage of accumulated moles in the back resin (with respect to the total accumulated moles) was around 29%, unambiguously indicating that some of the complexes in the river water were not fully labile. Indeed, for very labile complexes, the back percentage should be negligible because their dissociation (initiated along the diffusive gel) would have been completed within the front resin disc.

Taking into account VM speciation (see Table SI-2), confirmed by AGNES results, we split the total Zn concentration into the free fraction $[Zn^{2+}]$ and just an inorganic pool [ZnL]. Due to the small size of the inorganic complexes, one can assume the same diffusion coefficient as the free zinc: i.e. $\varepsilon_{ZnL} = 1$. So, Eq. (7) simplifies to:

$$c_{DGT} = \left[Zn^{2+}\right] + \xi_{DGT}[ZnL] \quad (17)$$

Thus, the lability degree of a particular configuration (ξ_{DGT}) can be computed from its c_{DGT}, the free concentration (e.g. from AGNES or another technique) and the concentration of the pool of complexes, which derives from the total concentration balance (i.e. $[ZnL] = c_{T,Zn} - [Zn^{2+}]$).

The obtained ξ_{DGT} values were 0.76 (1R1G), 0.84 (1R2G), and 0.94 (2R1G). Due to the time-average nature of DGT measurements, in this case the average total concentration (595 nmol L^{-1}) has been used for $c_{T,Zn}$. These lability degrees are self-consistent (details not shown) with the theoretical treatment around Eq. 6 in (Sans-Duñó et al., 2021) (with no electrostatic effect considered because of the majoritary complexes being uncharged, see SI) and lead to a kinetic dissociation constant $k_d = 2.68 \times 10^{-3}$ s^{-1} in good agreement with $k_d = 3.35 \times 10^{-3}$ s^{-1} obtained by introducing the abovementioned 29% back accumulation in Eq. 9 of reference (Jimenez-Piedrahita et al., 2015) which is also reproduced in SI-11 of the present work.

The relatively low lability degree found here for Zn complexes in the 1R1G device is consistent with the one that can be derived from data in (Price et al., 2021) at pH 8.3. Indeed, they reported $c_{DGT} = 0.64 \times c_{T,Zn}$ which becomes $c_{DGT} = 0.88 \times c_{T,Zn}$, when one considers a DBL thickness of 0.3 mm (as in this work) on top of the typical diffusion domain of 0.8 mm. With their reported $[Zn^{2+}] = 0.31 \times c_{T,Zn}$ and Eq. (17), one finds $\xi = 0.83$, in reasonable agreement with the value found here ($\xi = 0.76$).

4.4. Labile concentration with LASV: c_{LASV}

To relate concentrations to fluxes, it is convenient to define c_{LASV} as the hypothetical concentration of free metal that would yield the

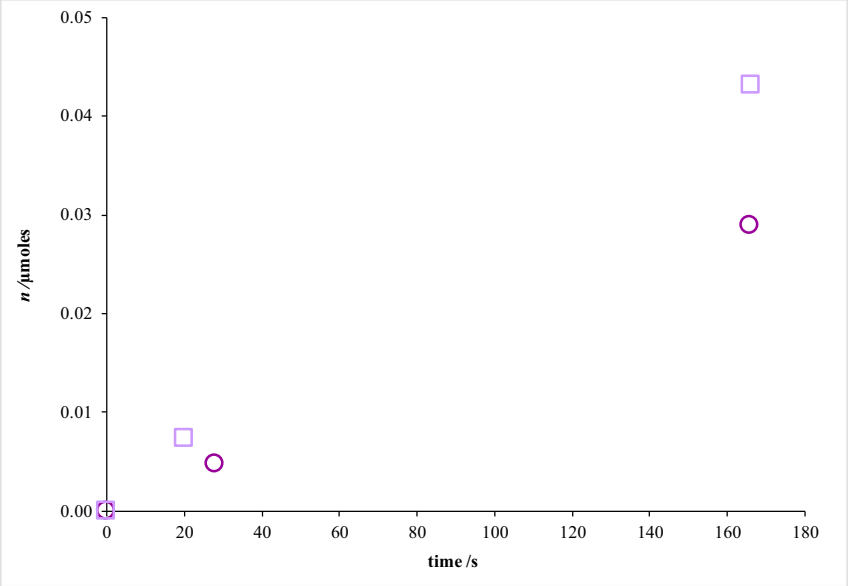

Fig. 2. Higher accumulation of Zn in DGT devices with 1 diffusive gel than with 2 diffusive gels at various sampling times. Light-purple squares stand for configuration 1R1G (one resin disc, one diffusive disc); dark-purple circles stand for configuration 1R2G (one resin disc, two diffusive discs).

same analytical response as the one actually found in the system (where there might be also complexes).

In the case of the RDE, for just one pool of Zn complexes, by combining this definition with Eqs. (9), (11) and (12), one obtains

$$c_{LASV} = \left[Zn^{2+}\right] + \xi_{LASV}\left(\left(\frac{\bar{D}}{D_{Zn}}\right)^{2/3} c_{T,Zn} - \left[Zn^{2+}\right]\right) \quad (18)$$

In the particular case of just one complex of Zn with the same mobility of the complexes as that of the free Zn cation (i.e. $\varepsilon = 1$), it simplifies to:

$$c_{LASV} = \left[Zn^{2+}\right] + \xi_{LASV}[ZnL] \quad (19)$$

This expression is parallel to c_{DGT} given by Eq. (17) and to the definition of the labile concentration for the technique DIET (Dynamic Ion Exchange Technique) (Quattrini et al., 2019)

$$c_{DIET} = \left[Zn^{2+}\right] + \varepsilon\xi_{DIET}[ZnL] \quad (20)$$

Thus, outcomes from DGT and LASV, which could initially be considered as merely "operationally defined" (Bourgeault et al., 2013; Cindric et al., 2020), have now (from Eqs. (17) and (19)) a well-defined meaning, which can be connected to physicochemical parameters *via* suitable modelling of the respective lability degrees (Baeyens et al., 2018; Galceran et al., 2021; Gao et al., 2019). Something alike happens with results from Chelex columns (Apte et al., 2005) to which Eq. (20) could be extended.

The computation of ξ_{LASV} in Osor water became particularly simple, because $\varepsilon = 1$ implied that the last multiplying factor in Eq. (15) reduced to just 1. Applying Eqs. (9), (11) and (15), $\xi_{LASV} = 0.090$ was obtained. From this value and with Eq. (19), $c_{LASV} = 155$ nmol L^{-1} resulted.

4.5. Integration of results

A first comparison (involving techniques providing equilibrium speciation) consists in checking the free Zn concentration retrieved by AGNES against that retrieved by PIM (whose methodology, modelling and results are reported in the Supporting Information). The final $[Zn^{2+}]$ determined with PIM (191 ± 99 nmol /L, see SI), leads to confirm the recently claimed capacity of PIM to determine free ion concentrations (Vera et al., 2018), as AGNES and PIM values agree within the reported standard deviations. One clear advantage of PIM over most AGNES implementations is its intrinsic capability for *in situ* deployment. As this work is the first application of PIM to *in situ* measure $[Zn^{2+}]$ in natural waters (and its deployment and interpretation could be considered as preliminary), while AGNES has a long tradition in this purpose (Galceran et al., 2007; Parat et al., 2015; Pearson et al., 2016), we have used AGNES-$[Zn^{2+}]$ in all further calculations where $[Zn^{2+}]$ was needed.

A second comparison of results (affecting the dynamic techniques) can focus on their quantification of the lability degree. A typical assertion in the literature is that the lability degree increases when the length of the diffusion path increases (Degryse and Smolders, 2016; van Leeuwen et al., 2005) and this is justified by stating that a longer path allows for a longer time to dissociate.

In the case of LASV, the diffusion length is the thickness of the diffusion layer $\bar{\delta}$ (see Eq. (14)), since $\varepsilon = 1$. For our RDE-TMF, $\bar{\delta} = \delta_{Zn}$ (from now on labelled δ_{LASV}) resulted 0.011 mm from the slope of the measured charges along a series of experiments with increasing deposition times, in a solution with just Zn and background electrolyte (see Eq. (4)). The value 0.011 mm resulted from three slopes of replicate experiments with different total Zn concentrations (7×10^{-7}, 2×10^{-6} and 7×10^{-6} mol L^{-1}). This δ_{LASV} could be reduced/increased by increasing/decreasing the RDE rotation speed (Hurst and Bruland, 2005) and was consistent with theoretical expectations (see Eq. (9.3.25) in reference (Bard and Faulkner, 2001)).

For DGT, there is diffusion along the DBL, the filter, the diffusive disc and –for partially labile complexes- also inside the resin disc. As the impact on dissociation in the resin domain is not the same as in the domain of the diffusive gel, we will define as characteristic length of DGT devices the thickness of the diffusive gel in an ideal DGT device, with no penetration at all in the resin (i.e. $\delta^r = 0$), which would sense the same accumulation (and, thus, the same lability degrees) as the real one. As commented above, from expression 6 in (Sans-Duñó et al., 2021) or SI-7, and the lability degree of 1R1G, $k_d = 2.68 \times 10^{-3}$ follows for

Osor water. On the other hand, this expression (also given in (Galceran and Puy, 2015)) simplifies to

$$\xi \approx 1 - \frac{\left(1 + K^{'}\right)}{K^{'} + \Delta g \sqrt{\frac{k_d(1+K')}{D_{Zn}}}} \tag{21}$$

when: i) $\varepsilon = 1$, ii) $\Delta g > 3 \times \sqrt{\frac{D_{Zn}}{k_d(1+K')}}$ (high lability degrees) and iii) there is no penetration of the complexes (i.e. $\delta^r = 0$). By solving for Δg in Eq. (21), we find the characteristic length Δg^c for DGT under these assumptions as

$$\Delta g^c = \left(\frac{1 + K^{'}}{1 - \xi} - K^{'}\right) \sqrt{\frac{D_{Zn}}{k_d(1 + K')}} \tag{22}$$

Now, with the lability degrees of the different types of devices, the characteristic lengths 3.2 (1R1G), 5.2 (1R2G) and 16.6 (2R1G) mm were found. The value 16.6 mm is likely to be an overestimation, perhaps due to the proximity of the lability degree to 1 (see denominator in Eq. (22)) and should be taken just as an estimate.

As seen in Fig. 3, the longer the path of the analyte towards the sensor, the more labile the pool complex becomes (Galceran et al., 2001). Since δ_{LASV} is very small, the lability degree is practically negligible ($\xi_{LASV} = 0.090$) in front of those measured for DGT (0.76, 0.84 and 0.94). If one considers δ_{LASV} completely negligible, it would mean that LASV would be measuring just the free metal ion plus very small and fully labile complexes (e.g. ion pairs). Among DGT lability degrees, the lowest corresponds to the configuration 1R1G, as expected. We also note that, in this instance, the adding to 1R1G of a thicker diffusive disc (to become 1R2G) has a less "labilizing" effect than the adding of a resin disc (to become 2R1G), because the resin disc drives locally to a very strong dissociation of the pool of complexes (see Fig. 3). The lability degrees found for the Zn pool of complexes (where $Zn(OH)_2$ is the dominant form) in this work with the various techniques (and other LASV experiments in synthetic $KNO_3 + Zn(NO_3)_2$ solutions at varying pH, not shown) and those in (Price et al., 2021) cannot be theoretically explained with a simple model based on Eigen mechanism (which would predict full lability for Zn hydroxides and carbonates), so that further work is required for a full understanding of this behaviour.

A third comparison (involving all techniques) focusses on the technique-dependent concentrations provided by the suite of sensors. They are collected in Fig. 4 ordered from the smallest one (the free fraction) to the largest one (the total concentration of Zn). In this particular water, due to the fact that $\varepsilon = 1$, the "maximum dynamic concentration" (Balistrieri and Blank, 2008; Bradac et al., 2009; Cindric et al., 2020; Davison and Zhang, 2012; Han et al., 2014; Macoustra et al., 2019; Unsworth et al., 2006), which is an upper limit to all dynamic techniques (by taking all lability degrees at their maximum value 1), coincides with the total concentration. Indeed, Eq. (17) becomes

$$c_{dyn}^{max} = \left[Zn^{2+}\right] + \varepsilon[ZnL] = \left[Zn^{2+}\right] + [ZnL] = c_{T,Zn} \tag{23}$$

Obviously (due to the equations of the effective concentrations in the various techniques with $\varepsilon = 1$) the order in Fig. 4 reflects the one in the lability degree.

The plot of Fig. 4 is the effective concentration signature of this water. On the one hand, the signature characterizes this kind of water and can be seen as a fingerprint that distinguishes it from all others (e.g. "site specific"). On the other hand, and more importantly, this signature can provide an estimation, usually by interpolation, of the maximum (i.e. if the biological internalization process is not limiting) available Zn that could be received by an organism in contact with this water from its diffusive characteristic length (Degryse and Smolders, 2016; van Leeuwen et al., 2005).

Let's consider, first, a couple of examples of the use of the effective concentration signature for benthic biota. The thickness of the diffusion layer (δ) for oxygen consumption of the photosynthesizing leaf of the freshwater macrophyte, *Vallisneria americana*, has been estimated as 0.151 mm, see Fig. 15.4 in (Nishihara and Ackerman, 2013). Assuming a similar δ for the maximum possible Zn uptake, it would mean that the leaf could be supplied –in this water- with an effective

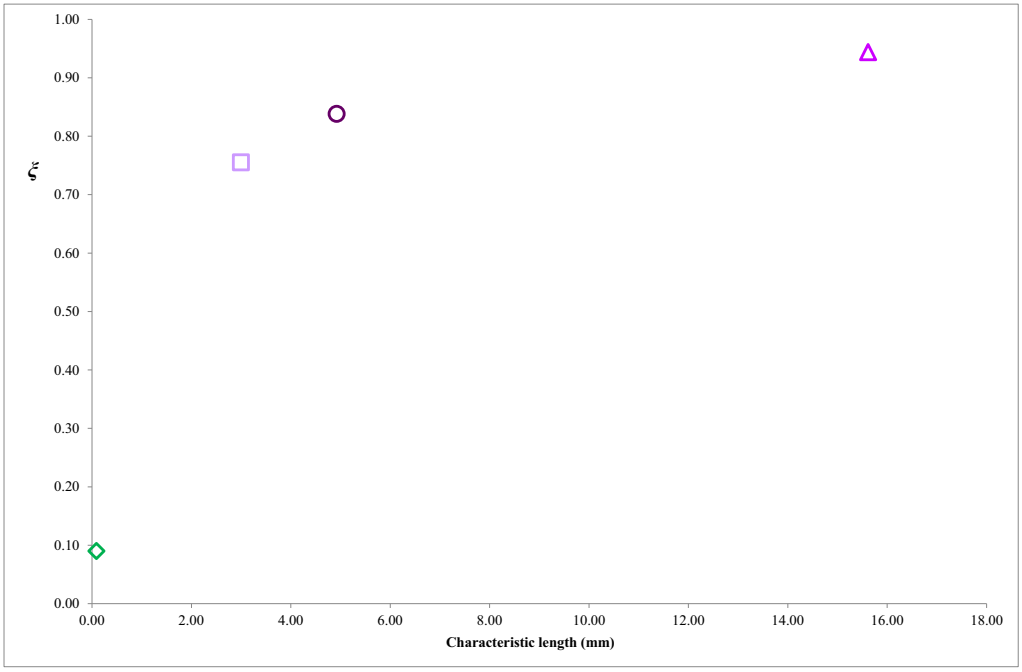

Fig. 3. Increased lability degrees of the Zn complex pool in Osor stream for higher characteristic lengths of the different techniques (LASV and DGT with various configurations) applied. Green diamond for LASV, light-purple square for 1R1G DGT, purple triangle for 2R1G and dark-purple circle for 1R2G.

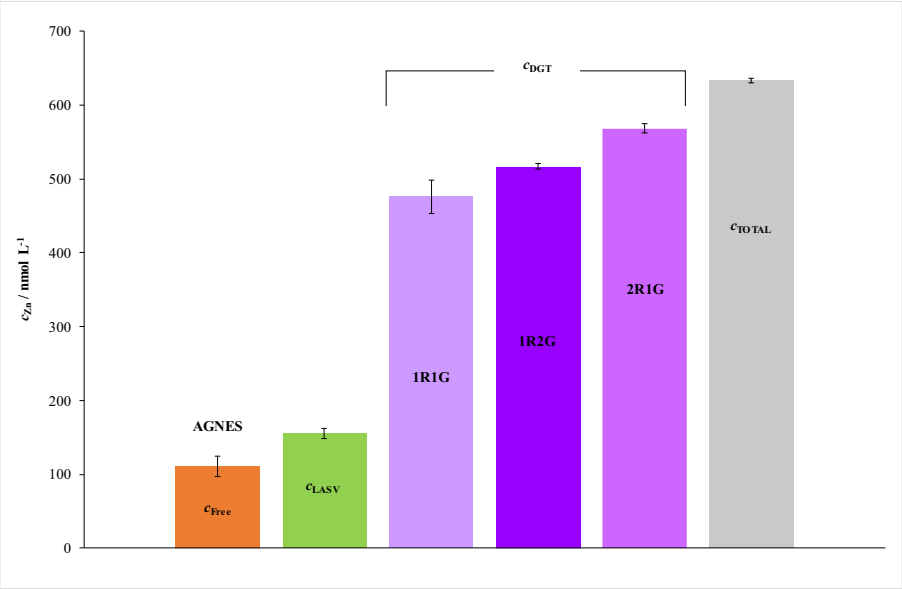

Fig. 4. Effective concentration signature for Zn in Osor stream including free, LASV-labile, DGT-labile (of different configurations) and total concentrations (ICP-MS). Error bars correspond to the standard deviation of the replicats.

concentration in between that of LASV (155 nmol L^{-1}) and that of DGT 1R1G (476 nmol L^{-1}). The diffusion boundary layer thickness for periphyton biolfilms is around 0.100 and 1.00 mm (Bradac et al., 2009; Degryse and Smolders, 2016), so that, again, in this water, the effective (maximum) concentration would be in between that of LASV and that of DGT 1R1G.

Let's consider, next, an example of the use of the effective concentration signature for pelagic biota. Microorganisms are surrounded by a diffusion boundary layer, where the taken up species is depleted, whose thickness, for assumed spherical organisms, coincides with the radius of these microorganisms (Degryse and Smolders, 2016; Fiksen et al., 2013; Nishihara and Ackerman, 2013). This happens because the size of the microorganism is below the Kolgomorov length and turbulences do not reach the microorganism, which tends to move with the main flow (Volker and Wolf-Gladrow, 1999). Given their few micron size (e.g 6.3 μm for *Prorocentrum minimum* or 1.5 μm for *Synechococcus* (Volker and Wolf-Gladrow, 1999), or many species of phytoplankton (Hurst and Bruland, 2005; Richardson and Stolzenbach, 1995)), one expects (from Figs. 3 and 4) an uptake much below that of LASV (155 nmol L^{-1}) and very close to the free concentration (111 nmol L^{-1}). This can be seen as another rationale for the fundamental tenet of the Free Ion Activity Model.

CRediT authorship contribution statement

Kevin Rosales-Segovia: Investigation, Writing – review & editing, Visualization. **Jordi Sans-Duñó:** Investigation, Software, Writing – review & editing. **Encarna Companys:** Resources, Writing – review & editing, Supervision. **Jaume Puy:** Conceptualization, Writing – review & editing. **Berta Alcalde:** Investigation, Writing – review & editing. **Enriqueta Anticó:** Resources, Writing – original draft, Writing – review & editing. **Clàudia Fontàs:** Conceptualization, Writing – review & editing. **Josep Galceran:** Conceptualization, Writing – original draft, Writing – review & editing, Project administration.

Declaration of competing interest

The authors declare that they have no known competing financial interests or personal relationships that could have appeared to influence the work reported in this paper.

Acknowledgments

Support from the Spanish Minister of Science and Innovation is gratefully acknowledged (Project PID2019-107033GB funded by MCIN/AEI/10.13039/501100011033). JSD acknowledges the University of Lleida for a fellowship PhD contract, and KRS his FISDUR grant (from Generalitat de Catalunya).

Appendix A. Supplementary data

Supplementary data to this article can be found online at https://doi.org/10.1016/j.scitotenv.2021.151201.

References

Almeida, M.I.G.S., Cattrall, R.W., Kolev, S.D., 2012. Recent trends in extraction and transport of metal ions using polymer inclusion membranes (PIMs). J. Membr. Sci. 415, 9–23.

Antico, E., Fontas, C., Vera, R., Mostazo, G., Salvado, V., Guasch, H., 2020. A novel cyphos IL 104-based polymer inclusion membrane (PIM) probe to mimic biofilm zinc accumulation. Sci. Total Environ. 715.

APHA, 1998. Indices indicating tendency of a water to precipitate CaCO3 or dissolve CaCO3. In: Clesceri, L.S., Greenberg, A.E., Eaton, A.D. (Eds.), Standard methods for the Examination of water and wastewater. Published jointly by American Public Health Association, American Water Works Association, Water Environment Federation, Washington DC 2-30-2-33.

Apte, S.C., Batley, G.E., Bowles, K.C., Brown, P.L., Creighton, N., Hales, L.T., et al., 2005. A comparison of copper speciation measurements with the toxic responses of three sensitive freshwater organisms. Environ. Chem. 2, 320–330.

Baeyens, W., Gao, Y., Davison, W., Galceran, J., Leermakers, M., Puy, J., et al., 2018. In situ measurements of micronutrient dynamics in open seawater show that complex dissociation rates may limit diatom growth. Sci. Rep. 8.

Balistrieri, L.S., Blank, R.G., 2008. Dissolved and labile concentrations of cd, cu, pb, and zn in the south fork Coeur d'Alene River, Idaho: comparisons among chemical equilibrium models and implications for biotic ligand models. Appl. Geochem. 23, 3355–3371.

Bard, A.J., Faulkner, L.R., 2001. Electrochemical methods. Fundamentals and applications. John Wiley & Sons Inc, New York.

Bourgeault, A., Ciffroy, P., Garnier, C., Cossu-Leguille, C., Masfaraud, J.F., Charlatchka, R., et al., 2013. Speciation and bioavailability of dissolved copper in different freshwaters: comparison of modelling, biological and chemical responses in aquatic mosses and gammarids. Sci. Total Environ. 452–453, 68–77.

Bradac, P., Behra, R., Sigg, L., 2009. Accumulation of cadmium in periphyton under various freshwater speciation conditions. Environ. Sci. Technol. 43, 7291–7296.

Chito, D., Weng, L., Galceran, J., Companys, E., Puy, J., van Riemsdijk, W.H., et al., 2012. Determination of free Zn2+ concentration in synthetic and natural samples with AGNES (Absence of gradients and Nernstian equilibrium Stripping) and DMT (Donnan membrane Technique). Sci. Total Envir. 421–422, 238–244.

Cindric, A.M., Marcinek, S., Garnier, C., Salaun, P., Cukrov, N., Oursel, B., et al., 2020. Evaluation of diffusive gradients in thin films (DGT) technique for speciation of trace metals in estuarine waters - a multimethodological approach. Sci. Total Environ. 721.
Companys, E., Cecília, J., Codina, G., Puy, J., Galceran, J., 2005. Determination of the concentration of free Zn2+ with AGNES using different strategies to reduce the deposition time. J. Electroanal. Chem. 576, 21–32.
Companys, E., Galceran, J., Pinheiro, J.P., Puy, J., Salaün, P., 2017. A review on electrochemical methods for trace metal speciation in environmental media. Curr. Opin. Electrochem. 3, 144–162.
Companys, E., Galceran, J., Puy, J., Sedo, M., Vera, R., Antico, E., et al., 2018. Comparison of different speciation techniques to measure Zn availability in hydroponic media. Anal. Chim. Acta 1035, 32–43.
Davison, W., Zhang, H., 1994. In-situ speciation measurements of trace components in natural- waters using thin-film gels. Nature 367, 546–548.
Davison, W., Zhang, H., 2012. Progress in understanding the use of diffusive gradients in thin films (DGT) – back to basics. Environ. Chem. 9, 1–13.
Degryse, F., Smolders, E., 2016. DGT and bioavailability. In: Davison, W. (Ed.), Diffusive Gradients in Thin-films for Environmental Measurements. Cambridge University Press, Cambridge, pp. 216–262.
Fiksen, Ø., Follows, M.J., Aksnes, D.L., 2013. Trait-based models of nutrient uptake in microbes extend the michaelis-menten framework. Limnol. Oceanogr. 58, 193–202.
Galceran, J., Puy, J., 2015. Interpretation of diffusion gradients in thin films (DGT) measurements: a systematic approach. Environ. Chem. 12, 112–122.
Galceran, J., Puy, J., Salvador, J., Cecília, J., van Leeuwen, H.P., 2001. Voltammetric lability of metal complexes at spherical microelectrodes with various radii. J. Electroanal. Chem. 505, 85–94.
Galceran, J., Companys, E., Puy, J., Cecília, J., Garcés, J.L., 2004. AGNES: a new electroanalytical technique for measuring free metal ion concentration. J. Electroanal. Chem. 566, 95–109.
Galceran, J., Huidobro, C., Companys, E., Alberti, G., 2007. AGNES: a technique for determining the concentration of free metal ions. The case of Zn(II) in coastal Mediterranean seawater. Talanta 71, 1795–1803.
Galceran, J., Lao, M., David, C., Companys, E., Rey-Castro, C., Salvador, J., et al., 2014. The impact of electrodic adsorption on Zn, Cd or Pb speciation measurements with AGNES. J. Electroanal. Chem. 722–723, 110–118.
Galceran, J., Gao, Y., Puy, J., Leermakers, M., Rey-Castro, C., Zhou, C., et al., 2021. Front. Chem. 9.
Gao, Y., Zhou, C.Y., Gaulier, C., Bratkic, A., Galceran, J., Puy, J., et al., 2019. Labile trace metal concentration measurements in marine environments: from coastal to open ocean areas. 116, 92–101.
Han, S.P., Zhang, Y., Masunaga, S., Zhou, S.Y., Naito, W., 2014. Relating metal bioavailability to risk assessment for aquatic species: Daliao River watershed,China. 189, 215–222.
Hurst, M.P., Bruland, K.W., 2005. The use of nafion-coated thin mercury film electrodes for the determination of the dissolved copper speciation in estuarine water. Anal. Chim. Acta 546, 68–78.
Jansen, R.A.G., van Leeuwen, H.P., Cleven, R.F.M.J., van den Hoop, M.A.G.T., 1998. Speciation and lability of zinc(II) in river waters. Environ. Sci. Technol. 32, 3882–3886.
Jimenez-Piedrahita, M., Altier, A., Cecilia, J., Rey-Castro, C., Galceran, J., Puy, J., 2015. Influence of the settling of the resin beads on diffusion gradients in thin films measurements. Anal. Chim. Acta 885, 148–155.
Lao, M., Dago, A., Serrano, N., Companys, E., Puy, J., Galceran, J., 2015. Free Zn2+ determination in systems with Zn-glutathione. J. Electroanal. Chem. 756, 207–211.
van Leeuwen, H.P., Town, R.M., Buffle, J., Cleven, R., Davison, W., Puy, J., et al., 2005. Dynamic speciation analysis and bioavailability of metals in aquatic systems. Environ. Sci. Technol. 39, 8545–8585.
Levy, J.L., Zhang, H., Davison, W., Galceran, J., Puy, J., 2012. Kinetic signatures of metals in the presence of Suwannee River fulvic acid. Environ. Sci. Technol. 46, 3335–3342.
Macoustra, G., Holland, A., Stauber, J., Jolley, D.F., 2019. Effect of various natural dissolved organic carbon on copper lability and toxicity to the tropical freshwater microalga Chlorella sp. Environ. Sci. Technol. 53, 2768–2777.
Menegario, A.A., Yabuki, L.N.M., Luko, K.S., Williams, P.N., Blackburn, D.M., 2017. Use of diffusive gradient in thin films for in situ measurements: a review on the progress in chemical fractionation, speciation and bioavailability of metals in waters. Anal. Chim. Acta 983, 54–66.
Monterroso, S.C.C., Carapuca, H.M., Duarte, A.C., 2003. Performance of poly (styrenesulfonate)-coated thin mercury film electrodes in the determination of lead and copper in estuarine water samples of high salinity. Electroanalysis 15, 1878–1883.
Morin, S., Corcoll, N., Bonet, B., Tlili, A., Guasch, H., 2014. Diatom responses to zinc contamination along a Mediterranean river. Plant Ecol. Evol. 147, 325–332.
Navarro, A., Font, X., Viladevall, M., 2015. Metal mobilization and zinc-rich circumneutral mine drainage from the abandoned mining area of Osor (Girona, NE Spain). Mine Water Environ. 34, 329–342.
Nghiem, L.D., Mornane, P., Potter, I.D., Perera, J.M., Cattrall, R.W., Kolev, S.D., 2006. Extraction and transport of metal ions and small organic compounds using polymer inclusion membranes (PIMs). J. Membr. Sci. 281, 7–41.
Nishihara, G.N., Ackerman, J.D., 2013. Mass transport in aquatic environments. In: Shiva, S.G., Gualtieri, C., Mihailovic, D.T. (Eds.), Fluid Mechanics of Environmental Interfaces. CRC Press, London, pp. 423–452.
Parat, C., Authier, L., Aguilar, D., Companys, E., Puy, J., Galceran, J., et al., 2011. Direct determination of free metal concentration by implementing stripping chronopotentiometry as second stage of AGNES. Analyst 136, 4337–4343.
Parat, C., Authier, L., Castetbon, A., Aguilar, D., Companys, E., Puy, J., et al., 2015. Free Zn2+ determination in natural freshwaters of the Pyrenees: towards on-site measurements with AGNES. Environ. Chem. 12, 329–337.
Pearson, H.B.C., Galceran, J., Companys, E., Braungardt, C., Worsfold, P., Puy, J., et al., 2016. Absence of gradients and Nernstian equilibrium stripping (AGNES) for the determination of [Zn2+] in estuarine waters. Anal. Chim. Acta 912, 32–40.
Pei, J.H., Tercier-Waeber, M.L., Buffle, J., 2000. Simultaneous determination and speciation of zinc, cadmium, lead, and copper in natural water with minimum handling and artifacts, by voltammetry on a gel-integrated microelectrode array. Anal. Chem. 72, 161–171.
Pesavento, M., Alberti, G., Biesuz, R., 2009. Analytical methods for determination of free metal ion concentration, labile species fraction and metal complexation capacity of environmental waters: a review. Anal. Chim. Acta 631, 129–141.
Pinheiro, J.P., van Leeuwen, H.P., 2001. Metal speciation dynamics and bioavailability. 2. Radial diffusion effects in the microorganism range. Environ. Sci. Technol. 35, 894–900.
Pinheiro, J.P., Galceran, J., Rotureau, E., Companys, E., Puy, J., 2020. Full wave analysis of stripping chronopotentiometry at scanned deposition potential (SSCP): obtaining binding curves in labile heterogeneous macromolecular systems for any metal-to-ligand ratio. J. Electroanal. Chem. 873.
Pohl, P., Saparov, S.M., Antonenko, Y.N., 1998. The size of the unstirred layer as a function of the solute diffusion coefficient. Biophys. J. 75, 1403–1409.
Price, G.A.V., Stauber, J.L., Holland, A., Koppel, D.J., Van Genderen, E.J., Ryan, A.C., et al., 2021. The influence of pH on zinc lability and toxicity to a tropical freshwater microalga. Environ. Toxicol. Chem. 40, 2836–2845.
Puy, J., Galceran, J., 2017. Theoretical aspects of dynamic metal speciation with electrochemical techniques. Curr. Opin. Electrochem. 1, 80–87.
Quattrini, F., Galceran, J., Rey-Castro, C., Puy, J., Fortin, C., 2019. Assessment of labilities of metal complexes with the dynamic ion exchange technique. Environ. Chem. 16, 151–164.
Richardson, L.L., Stolzenbach, K.D., 1995. Phytoplankton cell-size and the development of microenvironments. FEMS Microbiol. Ecol. 16, 185–191.
Rocha, L.S., Companys, E., Galceran, J., Carapuca, H.M., Pinheiro, J.P., 2010. Evaluation of thin mercury film rotating disc electrode to perform absence of gradients and nernstian equilibrium stripping (AGNES) measurements. Talanta 80, 1881–1887.
Rotureau, E., Pla-Vilanova, P., Galceran, J., Companys, E., Pinheiro, J.P., 2019. Towards improving the electroanalytical speciation analysis of indium. Anal. Chim. Acta 1052, 57–64.
Sans-Duñó, J., Cecilia, J., Galceran, J., Puy, J., 2021. Availability of metals to DGT devices with different configurations. The case of sequential Ni complexation. Sci. Total Environ. 779, 146277.
Serrano, N., Diaz-Cruz, J.M., Ariño, C., Esteban, M., 2003. Comparison of constant-current stripping chronopotentiometry and anodic stripping voltammetry in metal speciation studies using mercury drop and film electrodes. J. Electroanal. Chem. 560, 105–116.
Sierra, J., Roig, N., Papiol, G., Perez-Gallego, E., Schuhmacher, M., 2017. Prediction of the bioavailability of potentially toxic elements in freshwaters. Comparison between speciation models and passive samplers. Sci. Total Environ. 605, 211–218.
Sigg, L., Black, F., Buffle, J., Cao, J., Cleven, R., Davison, W., et al., 2006. Comparison of analytical techniques for dynamic trace metal speciation in natural freshwaters. Environ. Sci. Technol. 40, 1934–1941.
Sjostedt, C.S., Gustafsson, J.P., Kohler, S.J., 2010. Chemical equilibrium modeling of organic acids, pH, aluminum, and iron in Swedish surface waters. Environ. Sci. Technol. 44, 8587–8593.
Tolmachev, Y.V., Scherson, D.A., 1999. Electrochemical reduction of bisulfite in mildly acidic buffers: kinetics of sulfur dioxide bisulfite interconversion. J. Phys. Chem. A 103, 1572–1578.
Unsworth, E.R., Warnken, K.W., Zhang, H., Davison, W., Black, F., Buffle, J., et al., 2006. Model predictions of metal speciation in freshwaters compared to measurements by in situ techniques. Environ. Sci. Technol. 40, 1942–1949.
Vera, R., Fontàs, C., Galceran, J., Serra, O., Anticó, E., 2018. Polymer inclusion membrane to access Zn speciation: comparison with root uptake. Sci. Total Environ. 622–623, 316–324.
Volker, C., Wolf-Gladrow, D.A., 1999. Physical limits on iron uptake mediated by siderophores or surface reductases. Mar. Chem. 65, 227–244.
Warnken, K.W., Davison, W., Zhang, H., Galceran, J., Puy, J., 2007. In situ measurements of metal complex exchange kinetics in freshwater. Environ. Sci. Technol. 41, 3179–3185.
Worms, I., Simon, D.F., Hassler, C.S., Wilkinson, K.J., 2006. Bioavailability of trace metals to aquatic microorganisms: importance of chemical, biological and physical processes on biouptake. Biochimie 88, 1721–1731.
Zavarise, F., Companys, E., Galceran, J., Alberti, G., Profumo, A., 2010. Application of the new electroanalytical technique AGNES for the determination of free zn concentration in river water. Anal. Bioanal. Chem. 397, 389–394.
Zhao, J.J., Cornett, R.J., Chakrabarti, C.L., 2020. Assessing the uranium DGT-available fraction in model solutions. J. Hazard. Mater. 384.